Int. J. Simul. Multidisci. Des. Optim. **11**, 14 (2020)

https://doi.org/10.1051/smdo/2020010

IJSMDO
Available online at:
https://www.ijsmdo.org

RESEARCH ARTICLE OPEN ACCESS

Modeling of a square-shape ZnO, ZnS and AlN membrane for mems capacitive pressure-sensor applications

Ahmad Dagamseh[1,*], Qais Al-Bataineh[2], Zaid Al-Bataineh[1], Nermeen S. Daoud[2], Ahmad Alsaad[2], and Ahmad Omari[2]

[1] Electronics Engineering Department, Hijjawi Faculty for Engineering Technology, Yarmouk University, P.O. Box 21163, Irbid, Jordan
[2] Department of Physical Sciences, Jordan University of Science and Technology, P.O. Box 3030, Irbid 22110, Jordan

Received: 27 December 2019 / Accepted: 29 June 2020

Abstract. In this paper, mathematical modeling and simulation of a MEMS-based clamped square-shape membrane for capacitive pressure sensors have been performed. Three types of membrane materials were investigated (i.e. Zinc Oxide (ZnO), Zinc Sulfide (ZnS) and Aluminum Nitride (AlN)). Various performance parameters such as capacitance changes, deflection, nonlinearity, the sensitivity of the membrane structure for different materials and film-thicknesses have been considered using the Finite Element Method (FEM) and analytically determined using the FORTRAN environment. The simulation model outperforms in terms of the effective capacitance value. The results show that the membrane deflection is linearly related to the applied pressure. The ZnS membrane provides a capacitance of 0.023 pico-Farad at 25 kPa with a 42.5% relative capacitance changes to reference capacitance. Additionally, the results show that for ZnO and AlN membranes the deflection with no thermal stress is higher than that with thermal stress. However, an opposite behavior for the ZnS membrane structure has been observed. The mechanical and capacitance sensitivities are affected by the membrane thickness as the capacitance changes are inversely proportional to the membrane thickness. Such results open possibilities to utilize various materials for pressure sensor applications by means of the capacitance-based detection technique.

Keywords: ZnO / ZnS / AlN / capacitive pressure sensors / MEMS / COMSOL / FORTRAN

1 Introduction

Historically, pressure sensors have been receiving significant attention due to their potential for a variety of applications including the touch-sensitive on flexible displays [1,2], health-care condition monitoring [3], soft robotics [4], energy harvesting [5,6] and electronic skin [7,8]. Based on the transduction mechanism, pressure sensors can be mainly categorized into piezoelectric, piezoresistive and capacitive types [9].

1.1 Capacitive-based sensing principle

Generally, in MEMS technology the capacitor-based sensors are formed by suspending a mechanical structure (ex. a membrane or a cantilever) with integrated capacitor electrodes. The capacitor electrode is formed on top of the membrane with a fixed underlying electrode. The changes in the separation distance or the overlapping area between the integrated electrodes due to the applied pressure forces to the membrane cause a capacitance variation. These capacitance changes are related to the pressure and can be converted into an electrical signal via proper interfacing electronics [10].

In the literature, there have been great efforts to design and develop capacitive-based sensors for various applications. Bhol proposed in his paper design and modeling for the performance of a capacitive pressure sensor. The target was to improve the sensor sensitivity by means of optimizing the dimensions and the materials used in the sensor [11]. Kirankumar et al. in their paper provided an overview of the developments, design challenges, modeling, and analysis of MEMS-based pressure sensors [12]. Mishra et al. modeled capacitive pressure sensors using two different geometries (an elliptical and circular shapes) with the same electrode area [13]. From their simulation, the results show that elliptical-shaped capacitive pressure sensors have shown better linearity compared with the circular-membrane pressure sensor. Mishara et al. Performed modeling of capacitive sensors using the COMSOL Multiphysics simulator [14]. A detailed analysis of

* e-mail: a.m.k.dagamseh@yu.edu.jo

the stress behavior and its distribution were provided. Different shapes and material properties used in MEMS capacitive sensors have been investigated [15,16]. Shaikh et al. discussed in their paper the design of capacitive and piezoresistive pressure sensors [17]. The geometrical properties and design parameters were analyzed for improving the sensitivity of the sensors.

1.2 MEMS Technology

The current applications of the sensors require performing measurements with high resolution to quantify the characteristics of the stimulus. With the conventional sensors, there will be a need for high-density sensors fabricated in small size structures, which cannot be achieved with the typical sensor technologies. Hence, with the advances of MEMS (Microelectromechanical system) technology the fabrication of micro-scaled devices can be achieved.

MEMS technology integrates mechanical structures and electrical components to create devices in a wide-area of applications such as pressure sensors, accelerometers, gyroscopes, etc. [18]. This offers possibilities to fabricate light-weight, small-in-size, and high-density structures (benefiting from the enormous techniques used in MEMS) to improve the performance and reduce the costs of the traditional sensory systems. Additionally, the sensitivity of the sensor is improved using MEMS technology due to the high surface-area to volume-ratio and thereby high signal-to-noise ratio (SNR). MEMS emerged with the aid of the development of integrated circuit (IC) fabrication processes, in which sensors, actuators, and control functions are co-fabricated in silicon. With the possibility of integrating the interfacing circuitry at the sensor side, a fully functional smart-sensor can be obtained.

MEMS-based pressure sensors have attracted great attention for its small size, low cost, high performance, and high reliability [14]. Therefore, they have been used in pressure measurement in various environments. Specifically, the capacitive pressure sensors have been widely fabricated using MEMS technology due to high-pressure sensitivity, low noise and temperature sensitivity [14,19,20]. Additionally, for the capacitive-based sensors, the stress in the membranes has less effect on the transduction phenomenon when compared to piezoelectric and piezoresistive-base sensors. Moreover, to maximize the sensitivity of the piezo-based sensors the deposition of the piezo material should be accurate, which is for capacitive sensors a large tolerance is accepted.

1.3 Aims of the study

In microtechnology, aluminum nitride (AlN), zinc sulfide (ZnS) and zinc oxide (ZnO) are extensively utilized materials in a wide range of applications. These materials provide various outstanding properties such as piezoelectricity and pyroelectricity or elasto-optic and electro-optic effects [21–24].

This paper proposes a design of a MEMS-based capacitive pressure sensor with clamped square membrane utilizing three types of membrane materials; zinc oxide (ZnO), zinc sulfide (ZnS) and aluminum nitride (AlN) with air-cavity. A membrane-based pressure sensing mechanism is employed and analyzed in both analytical and simulation techniques, using FORTRAN and COMSOL Multiphysics.

2 Sensor analysis

Using MEMS technology, a square-shaped membrane was used to form the capacitance-based pressure sensor. Traditionally, the capacitor consists of two parallel plates of equal area A forming the capacitor electrodes separated with a distance d_0. The mathematical expression of the electrical capacitance of the two parallel plates is [16,25]:

$$C_0 = \varepsilon_0 \varepsilon_r \frac{A}{d_0} \tag{1}$$

where: ε_0 is the free space permittivity and equals 8.854×10^{-12} F m^{-1}, ε_r is the relative permittivity of the dielectric material between the capacitor electrodes, A is the area of overlap between the electrodes in meters squared (m^2), and d_0 is the separation between the electrodes on meters (m). After applied pressure on the upper plate, equation (1) cannot be used for determining the capacitance of the pressure sensor. For a square or circular membrane, the behavior is the same for applied pressure.

Due to the applied pressure, the acting force on the top electrode causes a deflection and thereby changes in the separation between two electrodes. For a square-shape membrane at x, y position, the deflection ($w(x, y)$) is given by the superposition of the deflection due to the applied pressure $w_1(x, y)$ and $w_2(x, y)$ due to the bending moments generated from the edge restrictions, both under simply supported edge conditions as described in equation (2) [26,27].

$$w(x, y) = w_1(x, y) + w_2(x, y). \tag{2}$$

Then the electrode deflection becomes as follows:

$$w_1(x, y) = \frac{4Pa^4}{D\pi^5} \sum_{m=1,3,5\ldots,\text{odd}}^{\infty} \frac{(-1)^{\frac{m-1}{2}}}{m^5} \cos(X) \times \left(1 - \frac{M \tanh(M)}{2\cosh(M)} \cosh(Y) + \frac{Y \sinh(Y)}{2\cosh(M)}\right). \tag{3}$$

$$w_2(x, y) = -\frac{4Pa^4}{D\pi^5} \sum_{m=1,3,5\ldots,\text{odd}}^{\infty} \times \left[e_m \times \frac{(-1)^{\frac{m-1}{2}}}{m^2 \cosh(M)} \times (S_1(X, Y) + S_2(X, Y))\right] \tag{4}$$

where

$$M = \frac{m\pi}{2}, X = \frac{m\pi x}{a}, Y = \frac{m\pi y}{a} \tag{5}$$

and

$$\begin{Bmatrix} S_1(X,Y) = \cos(X) \times [Y\sinh(Y) - M\tanh(M)\cosh(Y)] \\ S_2(X,Y) = \cos(Y) \times [X\sinh(X) - M\tanh(M)\cosh(X)] \end{Bmatrix} \tag{6}$$

The flexural rigidity D is given by the following equation [28]:

$$D = \frac{Eh^3}{12(1-v^2)} \tag{7}$$

where h is the membrane thickness; E is Young's modulus, v is Poisson's ratio [29].

Accordingly, at the center of the membrane (i.e. $x = a/2$ and $d = a/2$), the electrode deflection becomes:

$$w_{\max} = 0.00126\frac{a^4P}{D} = 0.001512\left(\left(1-v^2\right)\right)\frac{a^4P}{E\left(h^3\right)} \tag{8}$$

The mechanical sensitivity of the membrane is defined as the change in deflection with the change in pressure, which can be expressed as shown in equation (9) as:

$$S_m = \frac{dw}{dP}. \tag{9}$$

Then, the capacitance for the pressure sensor can be defined as shown in equation (10).

$$C_f = \varepsilon \iint \frac{\mathrm{d}x\mathrm{d}y}{d - w(x,y)}. \tag{10}$$

By using binomial expansion and replace D with equation (7), the capacitance of the pressure sensor using a square-shape membrane becomes [30]:

$$C = C_0\left(1 + \frac{12.5Pa^4}{2015dh}\right) \tag{11}$$

where d is the air gap, a is the length of membrane and C_0 is the zero-pressure capacitance; which can be defined as:

$$C_0 = \frac{0.4\varepsilon a^4}{d}. \tag{12}$$

Accordingly, the sensitivity of the capacitance-based pressure sensor is defined as the change in pressure with the change in capacitance, which for a square-shape membrane is given by:

$$S_c = \frac{\partial C}{\partial P} = C_0\left(\frac{1.25{a_0}^4}{2025dh}\right). \tag{13}$$

3 COMSOL multiphysics modeling

To model the pressure sensors using COMSOL Multiphysics, the capacitance pressure sensor Multiphysics interface has to be utilized. The Electro-mechanics interface is combined within the capacitance pressure sensors Multiphysics interface. The Electro-mechanics interface combines solid mechanics and electrostatics with a moving mesh to model the deformation of electrostatically actuated mechanical structures.

3.1 Geometric modeling

In this study, the geometry of the membrane pressure sensor was chosen as a square-shape membrane with various membrane thickness varying from 300 nm to 700 nm, as shown in Figure 1. Since the membrane is a symmetrical structure, a single quadrant of the membrane needs to be included in the model, provided using the symmetry boundary condition (see Fig. 2) [31–33]. The membrane contains a thin membrane held at a fixed potential of 1 V. The membrane is separated from the ground plane cavity sealed under a 2 μm thick air layer. The sides of the cavity are isolated to prevent any possible connection between the membrane and the ground plane. For the Electromechanics interface, the bottom electrode is considered fixed and the membrane is considered flexible.

3.2 Boundary conditions

The boundary condition for the deflection of the structure is limited to the z-axis direction. The ZnO, ZnS, or AlN/Air/Steel AISI 4340 are predefined materials in the COMSOL library. The Steel AISI 4340 alloy which is heat treatable and low alloy steel containing chromium, nickel and molybdenum are used as the base of the sensor. It has high toughness and strength in the heat-treated conditions [32]. Figure 3 shows a schematic representation for the structure of the materials of the capacitive pressure sensor. The material properties of the capacitive pressure sensor modeled in COMSOL are summarized in Table 1.

To solve the equations using the finite element method (FEM), the structure of the membrane pressure sensor was segmented into small areas (segments or "mesh"), as shown in Figure 4.

4 Results and discussion

In this paper, the deflection, capacitance, mechanical, and capacitance sensitivity for the proposed design of the capacitive pressure sensor were investigated. The sensor performance while varying the membrane thickness and membrane material was modeled using Finite Elements Method (FEM) simulation and FORTRAN analytical calculations.

Outside the sealed cavity, when the pressure changes the pressure difference causes a deflection in the membrane. Subsequently, the thickness of the air gap varies across the membrane and the capacitance to ground changes. The capacitance changes then can be determined by a proper interfacing circuit. Figure 5 shows the deflection profile for the ZnS membrane capacitance pressure sensor with 15 kPa applied pressure. The results show that, as expected, the maximum deflection occurs at the center of the membrane. The non-uniform potential on the vertical

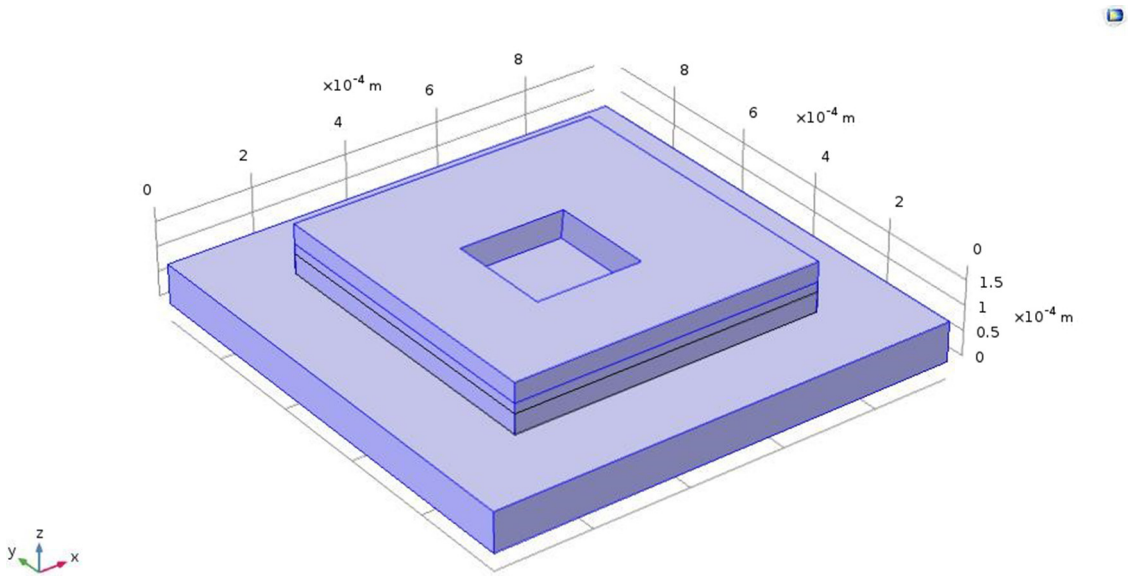

Fig. 1. The geometry of the square-shape capacitive pressure sensor.

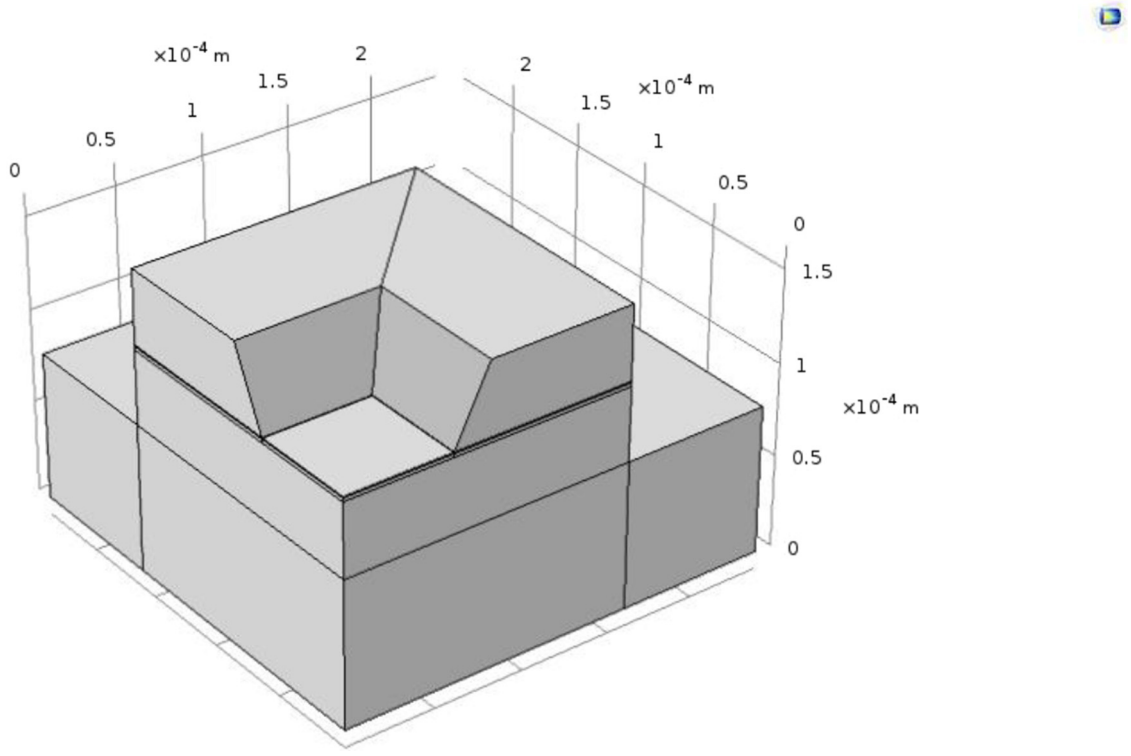

Fig. 2. The geometry of the capacitive pressure sensor modeled in COMSOL with one quadrant due to symmetry.

plane located between the plates of the capacitor is shown in Figure 6.

4.1 Effect of applied pressure

Figure 7 shows the average deflection of the membrane as a function of applied pressure. Three membrane materials (i.e. ZnO, ZnS, and AlN) have been investigated with no thermal stress at 500 nm membrane thickness. The results show that the average deflection increases while increasing the applied pressure with linear relation. To avoid pull-in conditions and to guarantee the linearity of the system, the maximum membrane deflection should not exceed 25% of the capacitor gap. On the other hand, among the three membrane materials, the ZnS has shown the highest deflection.

Table 1. Material properties of the capacitive pressure sensor.

Material type	Density kg/m^3	Young's modulus $\times 10^9$ Pa	Poisson's ratio	Coefficient of thermal expansion α $\times 10^{-6}$ 1/K
AlN	3300	326	0.25	5.0
ZnO	5676	210	0.33	2.9
ZnS	3980	74.5	0.28	6.5
Steel AISI 4340	7850	205	0.28	12.3

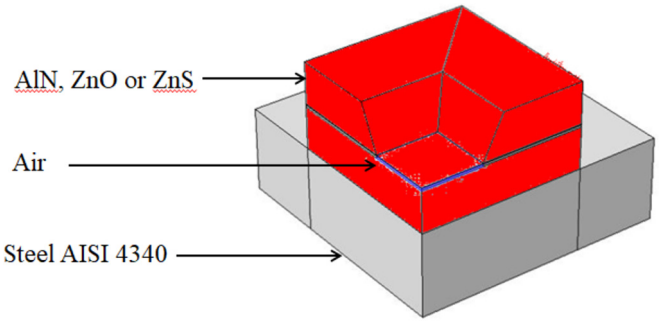

Fig. 3. The materials' structure of the capacitive pressure sensor.

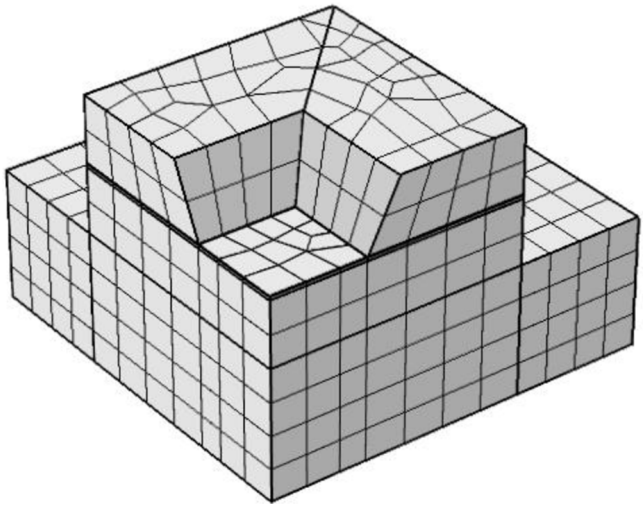

Fig. 4. Representation for the capacitive pressure sensor while showing the mesh points.

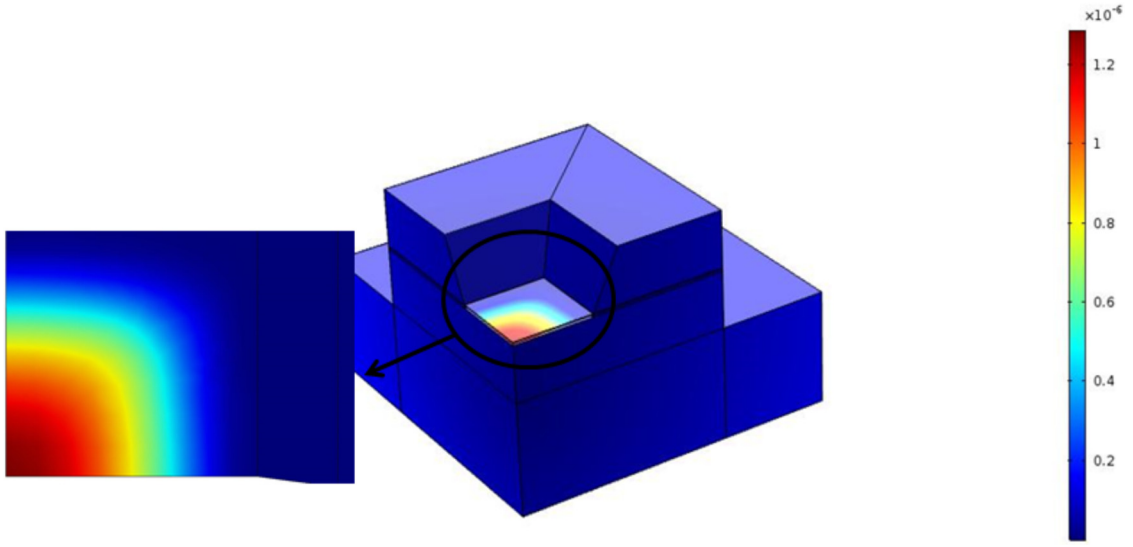

Fig. 5. Simulation for the deflection profile for 500 nm ZnS membrane thickness at 15 kPa applied pressure.

Based on the sensor design and principle of operation, the deformation of the membrane due to the applied pressure causes changes in capacitance [32]. Figure 8 shows the relative capacitance changes ($\Delta C/C_0$) for different membrane materials at various applied pressures. The results show that the capacitance increases linearly with the applied pressure. Belavic et al. and Lee et al. studied the linearity relation between the capacitance at various pressures. They related the sudden change in capacitance to the large displacement of the membrane

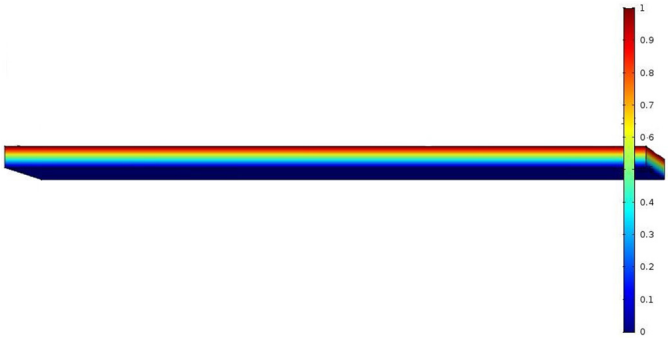

Fig. 6. Simulation for the potential along the ZnS membrane with a thickness of 500 nm at 15 kPa applied pressure.

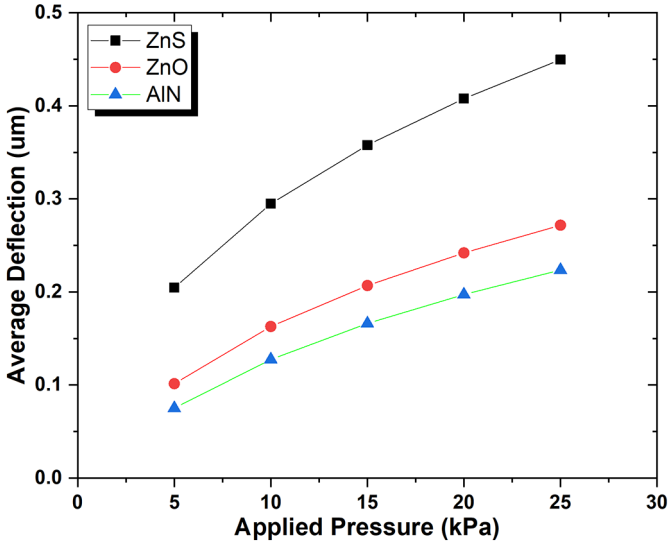

Fig. 7. The average deflection for different membrane materials with no thermal stress at different applied pressures.

at the applied pressure values due to the mechanical properties of the material [32,33].

The capacitance at zero-applied pressure for the three membrane materials is almost the same and equal to 15.9 fF. Therefore, the zero-pressure capacitance is independent of the membrane material type. The results show that the ZnS membrane provides the highest relative capacitance changes with 42.5% at 25 kPa applied pressure, compared with 19% and 14.5% for the ZnO and AlN structures, respectively. Figure 9 shows the simulated and calculated relative capacitance changes at various applied pressure values for a square-shape membrane using equation (11). It can be observed that the analytical results are close to the simulation results.

4.2 Effect of thermal stress

The deflection of the membrane is a result of the applied pressure and the complex interaction between the thermal stresses and the stresses introduced as a result of the applied pressure has resulted in both an initial offset

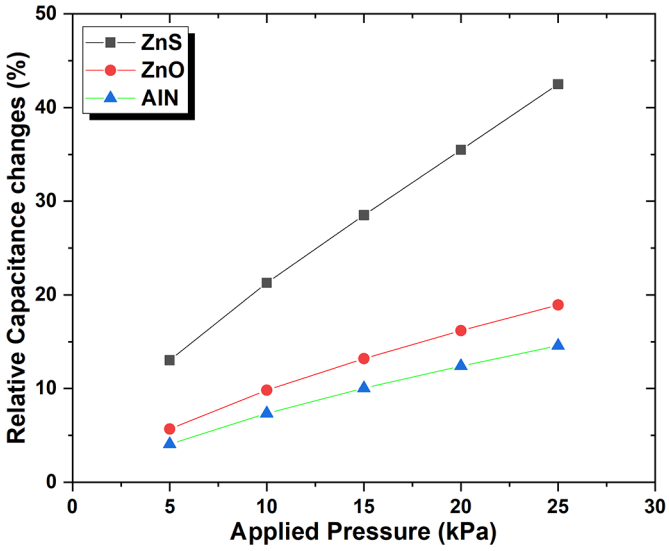

Fig. 8. The relative capacitance changes for various membrane materials with no thermal stress at different applied pressures.

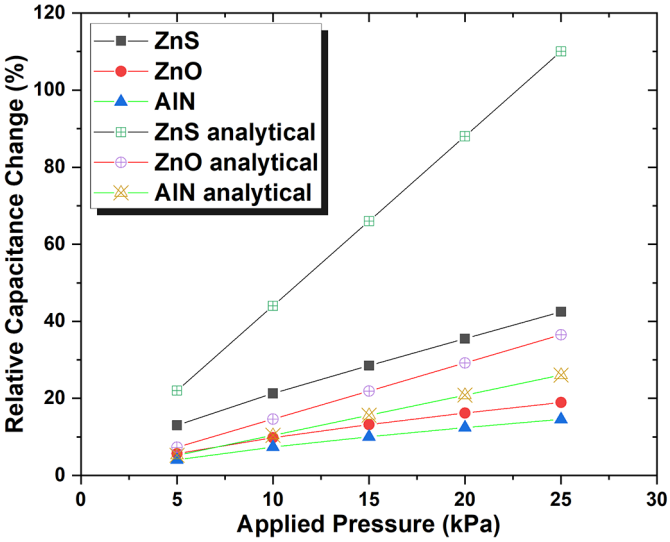

Fig. 9. The simulated and calculated relative capacitance changes for different membrane materials for a capacitive pressure sensor.

displacement and an increased dependence of the displacement on the pressure. Figure 10 shows the average deflection of 500 nm thick membrane with the applied pressure for different materials ZnO, ZnS, and AlN while considering the effect of thermal stress. The results show that for ZnO and AlN membranes the deflection with no thermal stress is higher than that with thermal stress. The lower deflection can be related to the reduced internal stress in the membranes. On the other hand, the ZnS membrane structure showed the opposite behavior. Accordingly, the capacitance of the membrane will be sensitive to thermal stress (see Fig. 11). The sensor sensitivity improves for structures exposed to thermal stress [32].

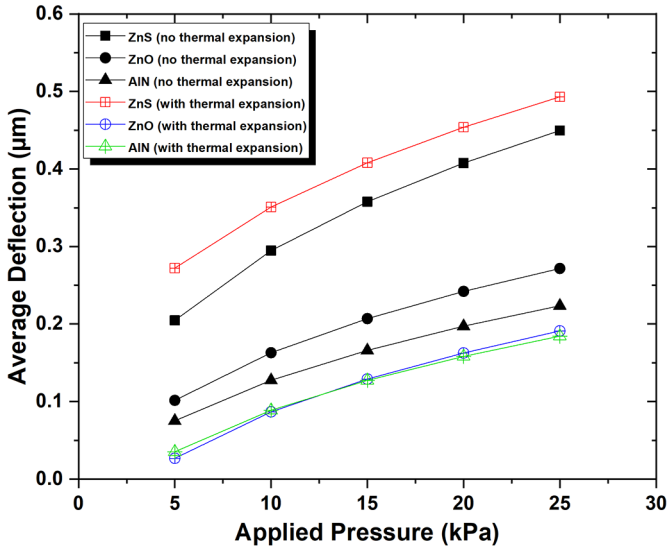

Fig. 10. The effect of thermal stress on the average deflection for various membrane materials.

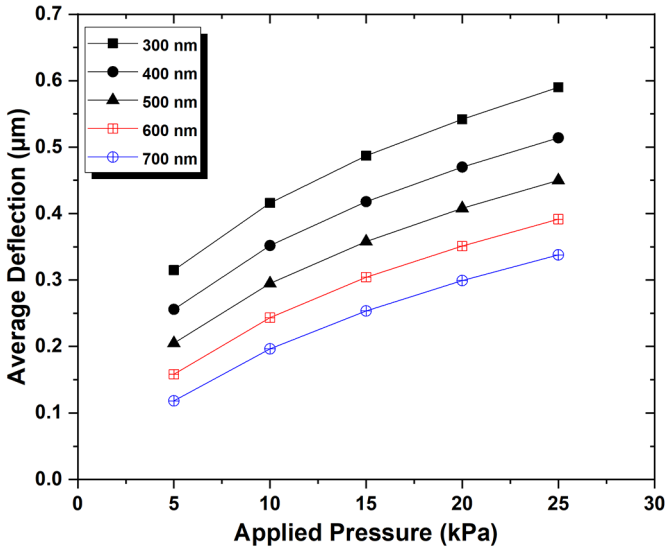

Fig. 12. The average deflection for different ZnS membrane thicknesses.

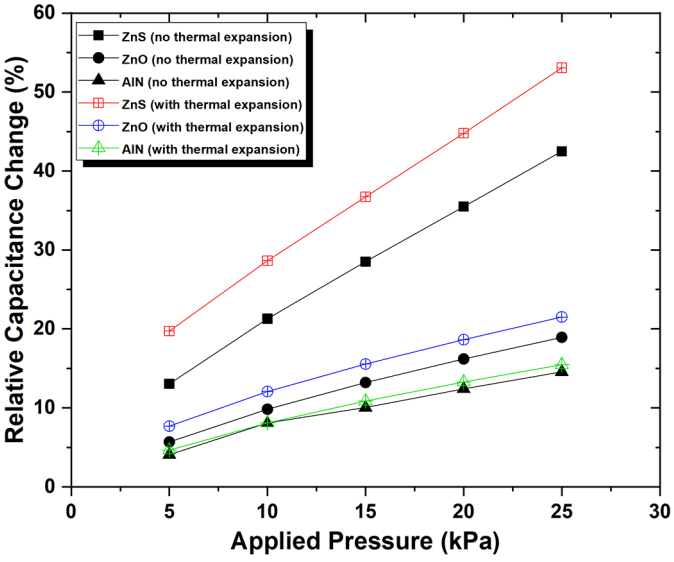

Fig. 11. The effect of thermal stress on the relative capacitance changes for different membrane materials.

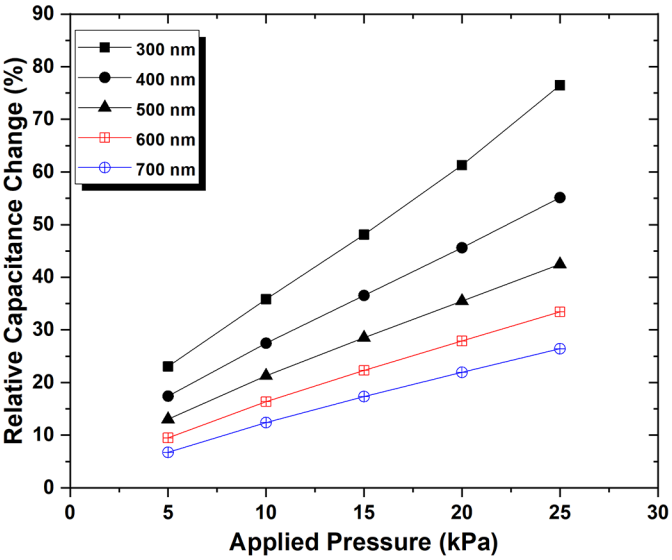

Fig. 13. The relative capacitance changes for different ZnS membrane thicknesses.

4.3 Effect of membrane thickness

Figure 12 shows the average deflection of the ZnS membrane as a function of applied pressure for different membrane thicknesses (i.e. 300 nm, 400 nm, 500 nm, 600 nm, and 700 nm) at the same separation gap of 2 µm. The results show that the average deflection is proportional to the applied pressure (as expected) and the reversely proportional to the film thickness. All three membrane materials have shown good linearity with a linear fit of $R^2 > 0.97$. The ZnS membrane with 300 nm thickness has shown the highest deflection with ~0.5 µm at 15 kPa applied pressure compared with ~0.25 µm for the membrane thickness of 700 nm. This can be related to the increase in the membrane mass and thereby the mechanical properties of the structure [34]. Therefore, if the membrane is thin the deflection is large as the stiffness of the structure is low. On the other hand, the 700 nm membrane thickness has shown the best linearity while the 300 nm has the best deflection and thereby more sensitive. Figure 13 shows the relation between the relative capacitance change and the applied pressure of the ZnS membrane.

To investigate the sensitivity of the membrane structure to the film thickness, equations (9) and (13) were used to determine the slopes of the curves in Figures 14 and 15. The results show that the membrane sensitivity to deflection depends inversely on the film thickness. This can be related to the mechanical behavior of the structure in such that the membrane becomes less elastic when increasing the thickness and while maintain-

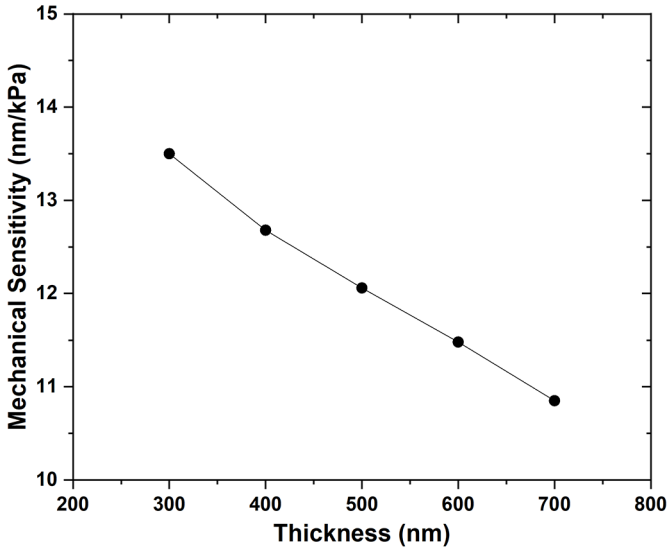

Fig. 14. The mechanical sensitivity of the sensor as a function of thickness for the ZnS membrane.

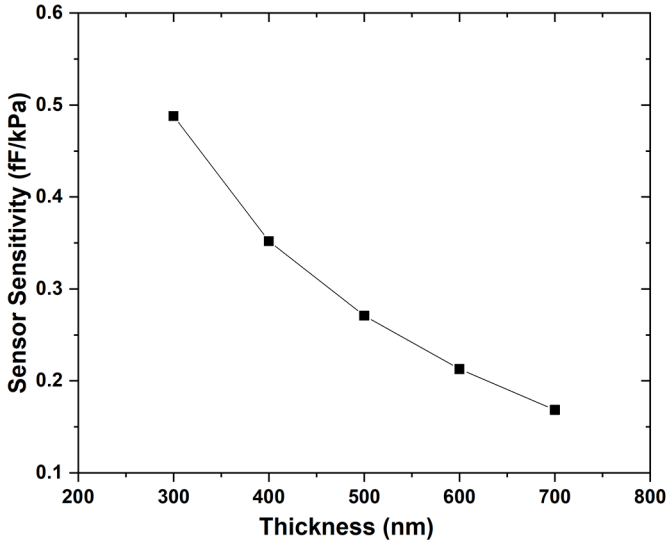

Fig. 15. The sensor sensitivity as a function of ZnS membrane thickness.

ing the same size [16]. This reveals a trade-off between sensor linearity and sensitivity. Accordingly, the ZnS membrane material has shown the best performance (in terms of sensor sensitivity and relative capacitance changes) with the 300 nm membrane thickness. Figures 14 and 15 show the relationship between the membrane thickness together with the mechanical and sensor sensitivities, respectively.

5 Conclusions

In this paper, a membrane-based capacitive pressure sensor was investigated analytically and simulated using the COMSOL Multiphysics simulator. Three types of membrane materials: AlN, ZnO, and ZnS with a structure of AlN/ZnO/ZnS-Air-Steel AISI 4340 have been considered. The average deflection of the membrane, relative capacitance changes, and sensor sensitivity as a function of applied pressure have been considered to represent sensor performance. The results show that the average deflection is linearly related to the applied pressure. Among the three investigated materials, the ZnS membrane has shown a higher deflection when compared with the ZnO and AlN membrane, using the same simulation conditions. The ZnS membrane has shown a 42.5% relative capacitance changes at 25 kPa applied pressure. Moreover, the results showed that the capacitance changes are inversely proportional to the membrane thickness and thereby the mechanical and capacitance sensitivities. Therefore, the least membrane thickness provides the maximum capacitance value.

References

1. D.J. Lipomi, M. Vosgueritchian, B.C. Tee, S.L. Hellstrom, J.A. Lee, C.H. Fox, Z. Bao, Skin-like pressure and strain sensors based on transparent elastic films of carbon nanotubes, Nat. Nanotechnol. **6**, 788 (2011)
2. F.R. Fan, L. Lin, G. Zhu, W. Wu, R. Zhang, Z.L. Wang, Transparent triboelectric nanogenerators and self-powered pressure sensors based on micropatterned plastic films, Nano Lett. **12**, 3109–3114 (2012)
3. C. Pang, G.Y. Lee, T.I. Kim, S.M. Kim, H.N. Kim, S.H. Ahn, K.Y. Suh, A flexible and highly sensitive strain-gauge sensor using reversible interlocking of nanofibres, Nat. Mater. **11**, 795 (2012)
4. S. Bauer, S. Bauer-Gogonea, I. Graz, M. Kaltenbrunner, C. Keplinger, R. Schwödiauer, A soft future: from robots and sensor skin to energy harvesters, Advanced Materials **26**, 149–162 (2014)
5. Z.L. Wang, W. Wu, Nanotechnology-enabled energy harvesting for self-powered micro-/nanosystems, Angew. Chem. In t. Ed. **51**, 11700–11721 (2012)
6. G. Zhu, W.Q. Yang, T. Zhang, Q. Jing, J. Chen, Y.S. Zhou, Z.L. Wang, Self-powered, ultrasensitive, flexible tactile sensors based on contact electrification, Nano Lett. **14**, 3208–3213 (2014)
7. J.W. Jeong, W.H. Yeo, A. Akhtar, J.J. Norton, Y.J. Kwack, S. Li, H. Cheng, Materials and optimized designs for human-machine interfaces via epidermal electronics, Adv. Mater. **25**, 6839–6846 (2013)
8. M. Kaltenbrunner, T. Sekitani, J. Reeder, T. Yokota, K. Kuribara, T. Tokuhara, S. Bauer, An ultra-lightweight design for imperceptible plastic electronics, Nature **499**, 458 (2013)
9. S.-Y. Liu, J.-G. Lu, H. Shieh, Influence of permittivity on the sensitivity of porous elastomer-based capacitive pressure sensors, IEEE Sens. J. **18**, 1870–1876 (2018)
10. N. Anadkat, M. Rangachar, Simulation based analysis of capacitive pressure sensor with COMSOL multiphysics, in International Journal of Engineering Research and Technology (ESRSA Publications, 2015)
11. K. Bhol, Highly sensitive MEMS based capacitive pressure sensor design using COMSOL multiphysics & its application in lubricating system, Eng. Appl. Sci. **2**, 66–71 (2017)

12. B. Kirankumar, B.G. Sheeparamatti, A critical review on MEMS capacitive pressure sensors, Sens. Transduc. J. **187**, 120–128 (2015)
13. R. Mishra, K. Kumar, Mathematical modelling and comparative study of elliptical and circular capacitive pressure microsensor, IOP Conf. Ser.: Mater. Sci. Eng. **404**, 012026 (2019)
14. G. Mishra, N. Paras, A. Arora, P.J. George, Simulation of MEMS based capacitive pressure sensor using comsol multiphysics, Int. J. Appl. Eng. Res. 7 (2012)
15. A. Sabet, X.J. Avula, Sensitivity to Shape and Membrane Thickness Variations in Capacitive Pressure Sensors, in *Technical Proceedings of the 2006 NSTI Nanotechnology Conference and Trade Show*, 2006
16. B.A. Ganji, M. Nateri, Modeling of capacitance and sensitivity of a MEMS pressure sensor with clamped square diaphragm, Int. J. Eng. Trans. B **26**, 1331–1336 (2013)
17. M.Z. Shaikh, S. Kodad, B. Jinaga, A comparative performance analysis of capacitive and piezoresistive MEMS for pressure measurement, Int. J. Comput. Sci. Appl. **1**, 201–204 (2008)
18. S. Saxena, R. Sharma, B. Pant, Design and development of guided four beam cantilever type MEMS based piezoelectric energy harvester, Microsyst. Technolog. **23**, 1751–1759 (2016)
19. M.A. Varma, S. Jindal, Novel design for performance enhancement of a touch-mode capacitive pressure sensor: theoretical modeling and numerical simulation, J. Comput. Electr. **17**, 1–10 (2018)
20. W.H. Ko, Q. Wang, Touch mode capacitive pressure sensors for industrial applications, in *Proceedings of Tenth Annual International Workshop on Micro Electro Mechanical Systems, MEMS' 97, IEEE*, 1997
21. M. Akiyama, K. Nagao, N. Ueno, H. Tateyama, T. Yamada, Influence of metal electrodes on crystal orientation of aluminum nitride thin films, Vacuum **74**, 699–703 (2004)
22. M. Shampa, Preparation of undoped and some doped ZnO thin films by silar and their characterization, Ph.D. thesis, The University of Bardhaman, 2013
23. P. Mackwitz, M. Rüsing, G. Berth, A. Widhalm, K. Müller, A. Zrenner, Periodic domain inversion in X-cut single-crystal lithium niobate thin film, Appl. Phys. Lett. **108**, 152902 (2016)
24. J. Cheng, D. Fan, H. Wang, B. Liu, Y. Zhang, H. Yan, Chemical bath deposition of crystalline ZnS thin films, Semicond. Sci. Technol. **18**, 676 (2003)
25. S.P. Timoshenko, S. Woinowsky-Krieger, Theory of plates and shells (McGraw-Hill, 1959)
26. S.-C. Gong, C. Lee, Analytical solutions of sensitivity for pressure microsensors, IEEE Sens. J. **1**, 340–344 (2001)
27. A. Ibrahim, Remotely interrogated MEMS pressure sensor, University of Glasgow, 2012
28. R. Khakpour, S.R. Mansouri, A. Bahadorimehr, Analytical comparison for square, rectangular and circular diaphragms in MEMS applications, in *Intl Conf on Electronic Devices, Systems and Applications (ICEDSA), IEEE*, 2010
29. K.B. Balavalad, B. Sheeparamatti, Sensitivity analysis of MEMS capacitive pressure sensor with different diaphragm geometries for high pressure applications, Young **1**, 1 (2015)
30. N. Anadkat, M. Rangachar, Simulation based analysis of capacitive pressure sensor with COMSOL multiphysics, Int. J. Eng. Res. Technol. **4**, 848–852 (2015)
31. A.E. Kubba, A. Hasson, A.I. Kubba, G. Hall, A micro-capacitive pressure sensor design and modelling, J. Sens. Sens. Syst. **5**, 95–112 (2016)
32. H.-S. Lee, S.P. Chang, C. Cho, Design and analysis of laminated stainless steel membrane-based microsensors, Sensors J. IEEE **8**, 182–187 (2008)
33. D. Belavič, M. Santo Zarnik, C. Marghescu, C. Ionescu, P. Svasta, M. Hrovat, S. Kocjan, Design of a capacitive LTCC-based pressure sensor, in *15th International Symposium for Design and Technology of Electronics Packages (SIITME)*, 2009, IEEE

Cite this article as: Ahmad Dagamseh, Qais Al-Bataineh, Zaid Al-Bataineh, Nermeen S. Daoud, Ahmad Alsaad, Ahmad Omari, Modeling of a square-shape ZnO, ZnS and AlN membrane for mems capacitive pressure-sensor applications, Int. J. Simul. Multidisci. Des. Optim. **11**, 14 (2020)